Biol Reprod. Author manuscript; available in PMC 2011 August 19.

Published in final edited form as:
Biol Reprod. 2003 February ; 68(2): 543–552.

Novel RING Finger Protein OIP1 Binds to Conserved Amino Acid Repeats in Sperm Tail Protein ODF1[1]

Heather A. Zarsky, **Min Cheng**, and **Frans A. van der Hoorn**[2]
Department of Biochemistry and Molecular Biology, University of Calgary Health Sciences Centre, Calgary, Alberta, Canada T2N 4N1

Abstract

Outer dense fibers (ODFs) and the fibrous sheath (FS) are unique structures of the mammalian sperm tail. Recently, progress has been made in the molecular cloning of ODF and FS proteins, and because of this, questions addressing the morphogenesis and underlying protein network that make up sperm tail structures and their function can now be addressed. Using the N-terminal leucine zipper motif of the major ODF protein ODF1, we had previously isolated interacting proteins Odf2, Spag4, and Spag5. We report here a yeast two-hybrid strategy to isolate a novel rat testicular protein, OIP1, that binds to the evolutionarily conserved Cys-Gly-Pro repeats in the C-terminus of ODF1. OIP1 is expressed in round spermatids as well as in spermatocytes and several somatic tissues, albeit at a lower level. No expression was detectable in epididymis, heart, and smooth muscle. OIP1 protein localizes to the sperm tail in a pattern expected for an ODF1-interacting protein. OIP1 belongs to the family of RING finger proteins of the H2 subclass. Deletion of the putative RING motif significantly decreased binding to ODF1. Genomic analysis of rat *Oip1* and *Oip1* homologs indicates that *Oip1* is highly conserved. *Oip1* is subject to differential splicing and alternative polyadenylation events. It is interesting that *Oip1* mRNAs have been reported that lack the exon encoding the putative RING finger.

Keywords

developmental biology; gamete biology; gametogenesis; spermatogenesis; testis

INTRODUCTION

The structure of the mammalian spermatozoon has been well characterized. The sperm cell can be divided into three regions: the head, the connecting piece (neck), and the tail [1]. Besides the axoneme, the tail contains two unique structures, outer dense fibers (ODFs) and the fibrous sheath (FS) that are not found in cilia or other unicellular flagella [1]. ODFs of distinct cross-sectional profiles extend throughout the tail in association with the microtubule doublets of the axoneme. A mitochondrial sheath surrounds ODFs in the midpiece, whereas the FS surrounds and replaces ODFs 3 and 8 in the principal piece [1]. At

[1]An Operating Grant from the Canadian Institutes of Health Research to F.A.vdH. supported this work.

[2]Correspondence: Frans A. van der Hoorn, Department of Biochemistry and Molecular Biology, University of Calgary, 3330 Hospital Drive N.W., Calgary, AB, Canada T2N 4N1. FAX: 403 283 8727; fvdhoorn@ucalgary.ca.

the ultrastructural level, ODFs have a thin, striated cortical layer with an electron-dense inner medulla [1, 2]. ODFs have a high cysteine and proline content [2, 3]. Solubilization and isolation of ODFs in a number of species have shown six major polypeptides of 84, 80, 30, 27, 20, and 14.4 kDa and a number of minor polypeptides [2, 4, 5]. The function of ODFs remains to be determined but recent studies suggest that ODFs increase the tensile strength of the sperm tail, which may aid in its protection from shearing forces encountered during transport and ejaculation [6]. In addition, many sperm tail defects resulting in male infertility may be associated with the absence of one or more ODF proteins or its interacting proteins (Oko, personal communication).

The underlying molecular network of testicular proteins that make up the sperm tail is relatively unknown. So far, few components of ODFs and their associated proteins have been isolated and characterized. The first ODF component to be identified was the 27-kDa ODF1 protein (previously called RT7 [7], Odf27 [8, 9], and rts5/1 [10]). Analysis of ODF1 showed two potentially functional domains: the first is the N-terminal amphipathic α helix, which is reminiscent of the leucine zipper dimerization protein motif [7]. Use of the ODF1 N-terminal leucine zipper as bait in protein interaction screens resulted in the isolation of several sperm tail proteins. One of these, Odf2 (formerly called Odf84 [11]), localizes to the connecting piece and both the cortex and medulla of the ODF [12]. Unlike the medullar expression of ODF1, cortical localization of Odf2 suggests that it can act as a structural link between the inner and outer regions of the ODFs. Recent data show that Odf2 is also a minor general scaffold protein of centrosome matrices in somatic cells [13]. We also isolated the ODF1-interacting proteins Spag4 [14] and Spag5 [15]. Spag4 is a 49-kDa protein that localizes to two microtubule-containing structures in male germ cells, the axoneme and the manchette. Spag4 is predominantly transcribed in round spermatids and is translated in elongating spermatids, and may serve to position the developing ODFs by acting as the first bridge between the axoneme and the ODF [14]. Spag5 encodes a 200-kDa protein with 73% similarity to the mitotic spindle protein Deepest. Spag5 is transcribed in pachytene spermatocytes and spermatids [15]. Spag4 and Spag5 strongly interact with ODF1 and have the ability to self-interact, but neither can associate with Odf2 [15]. All novel proteins contain one or two leucine zippers, one of which interacts with ODF1, and we propose that the leucine zipper is a common motif involved in specific protein-protein interactions in sperm tails [15].

The second ODF1 structural feature is a C-terminal Cys-Gly-Pro (CGP) repeat [16], also present in the *Drosophila Mst(3)* CGP gene family [17–19]. The *Mst(3)* gene family is composed of seven genes, five small genes of similar size and exon-intron structure (*Mst87F, Mst84Da, Mst84Db, Mst84Dc,* and *Mst84Dd*) and two tandemly arranged genes (*Mst98Ca* and *Mst98Cb*), which are much larger in size and contain no introns [19]. These mRNAs are exclusively expressed in the male germ line and are subject to translation control [17–19]. The *Mst(3)* gene family encodes proteins specific for the *Drosophila* sperm tail satellite fibers, which have been suggested to be functional homologs of mammalian sperm tail ODFs [18]. Deletion of the *Mst84D* gene members results in a 2-fold decrease in the number of functional sperm [19]. The two large genes are mostly composed of CGP repeats clustered at the C-terminus of the protein. The smaller proteins contain variable numbers of CGP and CCGP repeats [19]. Antibodies against *Mst98C* proteins show that

these genes are highly conserved throughout all species of *Drosophila* [19]. It is interesting that when *Mst87F* was used as a probe, the rat ODF1 gene (rts 5/1) was isolated [10].

To enhance our understanding of protein interactions within the sperm tail and to investigate the possibility that the conserved ODF1 CGP repeats interact with other sperm tail proteins, we used the ODF1 C-terminal portion in a yeast two-hybrid screen. Here we report the isolation and characterization of a novel rat testicular ODF1-interacting protein (OIP1). OIP1 sequence analysis suggests that it is a member of the RING finger family of proteins. Interaction studies using a RING finger deletion of OIP1 underscore the importance of this motif in protein-protein associations. The protein localizes to sperm tails. Gene expression analysis shows that OIP1 is predominantly but not exclusively expressed in spermatids and that it is first detected in testis at 10 days after birth.

MATERIALS AND METHODS

Library Construction and Screening

The construction of the testicular pGAD/cDNA expression library and λgt11 testicular cDNA expression library has been described [11]. The yeast two-hybrid screening procedures, including yeast transformation, β-galactosidase activity filter assay, plasmid DNA isolation and preparation, and false-positive elimination, have been described previously [11].

Yeast Cotransformations and OIP1 Expression Constructs

Yeast transformations were carried out in the HF7c yeast strain. Colonies of HF7c were inoculated into 10 ml of YPD medium and shaken overnight at 30°C. One-half milliliter of the culture was spun for 10 sec in a microcentrifuge, the supernatant was poured off, and 100 μg of salmon sperm carrier DNA and 10 μg of each transforming DNA were added. One-half milliliter of PLATE buffer (40% PEG 4000, 100 mM lithium acetate, 10 mM Tris-HCl pH 7.5, and 100 μM EDTA) was added and cells were mixed by vortexing. The tubes were incubated overnight at room temperature. Cells were gently mixed and 100 μl of the transformation mixture was spread onto 100 mm plates containing the appropriate synthetic selection media ($Leu^{-}Trp^{-}$ or $Leu^{-}Trp^{-}His^{-}$ selection plates). Plates were allowed to incubate at 30°C for 2–3 days. Plasmids in growing colonies were then characterized. One of these colonies contained plasmid pGAD18-8-1, which harbored the original rat testicular *OIP1* cDNA insert. The sequence of the pGAD18-8-1 insert was determined. pGAD18-8-1 was used as template in the Expand Long Template polymerase chain reaction (PCR) System (Roche Diagnostics, Laval, QC, Canada) to produce a RING finger *Oip1* deletion mutant as follows: two primers flanking the RING domain were designed to introduce *Eco*RI sites at the 5′ ends. PCR reactions were carried out with RING Pr-1 (5′-ACTGA-ATTCCAAAGTCTGCTCTGACTGG-3′) and RING Pr-2 (5′-ACTGA-ATTCCGAGCTATGCTTCTGAAG-3′). The PCR reaction profile was as follows: 92°C for 2 min, 3 cycles at 92°C for 12 sec, annealing at 58°C for 30 sec, and extension at 68°C for 6.5 min. An additional 27 cycles were carried out at 92°C for 12 sec, annealing at 65°C for 30 sec, and extension at 68°C for 6.5 min + 10 sec for each cycle; a final extension at 68°C for 7 min, and then cooling to 4°C. PCR products were analyzed on a 1% agarose gel,

isolated, purified, and digested with *Eco*RI, then self-ligated to generate the pGADΔRING construct. pGAD18-8-1 and p-GADΔRING were used in yeast two-hybrid transformations (as described above) in conjunction with pGBT9/ODF1 fragments obtained from Shao and van der Hoorn [9].

Cloning of OIP1 cDNA

PCR screening of the testicular λgt11 cDNA library—DNA isolated from the entire testicular phage λgt11 cDNA library [11] was used as template in PCR using the λgt11 forward primer (5′-GGTGGCGACGA-CTCCTGGAGCCCG-3′) and one of the following *Oip1*-specific reverse primers: RING Pr-1, RING Rev Pr (5′-CTGTGAGTCTCCGAGGCA-TAAATGG-3′), or Ig18-8-1 Pr (5′-0GGAGCTGACGGAGGTAATG-3′). The first PCR was carried out using 20 ng of λgt11 library DNA and 10 μM each of RING Pr-1 and λgt11 forward primer. PCR reaction products were analyzed on a 1% agarose gel and fragments greater than the predicted size, which contain additional 5′ sequences, were isolated and purified. These were next subjected to two rounds of seminested PCR. Bands were observed in the second and third seminested PCR, which were cloned in the pGEM-T-Easy vector (Promega, Madison, WI) and analyzed by sequencing in the DNA Sequencing Facility at the University of Calgary.

Reverse transcriptase-polymerase chain reaction of rat testis mRNA—We conducted a search using the basic alignment search tool (BLAST) database at the National Center for Biotechnology Information (NCBI; Bethesda, MD) to identify cDNAs related to rat *Oip1.* The human genome project database was used to identify the human chromosomal locus of *Oip1* and to predict a hypothetical gene structure with exon/intron boundaries for human OIP. The expressed sequence tag (EST) databases were searched to identify *Oip1*-related sequences. Several *Oip1*-related cDNAs were thus identified; one of these, mouse EST AK006888, was used to design a 5′ primer for use in rat testis reverse transcriptase (RT)-PCR. RT reactions were carried out using random primers as follows: the first-strand cDNA synthesis reactions contained 1 μg of round spermatid RNA, 1 μl of random primers (200 ng/μl), and diethyl pyrocarbonate-treated water to 11 μl and were heated to 70°C, then chilled on ice. Next, 4 μl of first-strand buffer was added together with 2 μl of 0.1 M dithiothreitol (DTT), 1 μl of dNTPs (10 mM each of dATP, dCTP, dTTP, and dGTP), and 1 μl of Superscript RT (Gibco, Invitrogen Corp., Burlington, ON, Canada). Reactions were carried out at 42°C for 1 h. Two microliters of cDNA was next used as PCR template together with forward primer 5′R-Mouse Cl Pr (5′-GACGAGACGCAGAGTGAAGATAG-3′) and reverse primer 5′ RACE RING Pr B (5′-GAAACGGATCACTAGAAATGAGG-3′). PCR products were gel-isolated, purified, cloned into the pDRIVE vector (Qiagen, Valencia, CA) and their sequences were analyzed. The completed rat testicular *Oip1* cDNA sequence was submitted to GenBank (accession number AF480444).

In Vitro Translation of OIP1

The pGAD18-8-1 insert was subcloned into the *Eco*RI/*Sal*I sites of a modified pBluescript KS^+ vector, pBS-ATG, which contains an ATG translation initiation codon inserted at the *Xba*I site [11]. The KS-ATG18-8-1 vector was then used as template in the Expand Long

Template PCR System (Boehringer-Mannheim) with RING Pr-1 and Pr-2 to obtain an *Oip1* construct with a RING finger deletion. In vitro translations were performed using the TNT Coupled Reticulocyte Lysate System (Promega) in the presence of [^{35}S]Met and carried out according to the manufacturer's protocols.

GST-ODF1 Fusion Constructs and Protein Production

The GST-ODF1 fusion constructs NT (N-terminal), ΔNT, CT (C-terminal), and ΔCT were described in [9]. NTΔzip was made by PCR using RT7-LZdel Pr (5′-GCAGGATCCAGATGTATCGACGAAATCAGCTC-3′) containing a *Bam*HI site and the T3 sequencing primer (5′-GCGCAAT-TAACCCTCACTAAAGG-3′). pRT7 [7] was used as the template. The PCR product was cut with *Bam*HI and the 366 base pair (bp) N-terminal portion was gel-isolated and ligated into pGEX-KG cut with *Bam*HI to produce pGEX-NT25–147. Clones with inserts in the correct orientation were identified by restriction analysis. Glutathione *S*-transferase (GST) fusion proteins were prepared essentially as described in [20]. A single colony of XL-1Blue (Stratagene, La Jolla, CA) transformed with the plasmid of interest was grown overnight in l ml of Luria broth (LB) containing 50 μg/ml ampicillin at 37°C with shaking. The overnight culture was added to 9 ml of fresh LB (1:10 dilution) containing 50 μg/ml ampicillin and grown for 2 h until the OD_{600} was 0.6–0.8. Protein synthesis was induced with 0.2 mM isopropyl-β-D-thiogalactopyranoside for 4 h at 37°C. Bacteria were pelleted and washed once with 2 ml of ice-cold STE (10 mM Tris-HCl pH 8.0, 150 mM NaCl, and 1 mM EDTA) and resuspended in 1.35 ml of STE containing 100 μg/ml of lysozyme (added immediately before resuspension) and incubated on ice for 15 min. DTT was added to a final concentration of 5 mM. Bacteria were lysed by addition of 1.5% *N*-lauryl sarcosine (sarkosyl). After vortexing, the cells were sonicated on ice for 2 min and centrifuged at full speed in a microfuge at 4°C for 10 min. The supernatant was transferred to a new Eppendorf tube. Triton X-100 was added to a final concentration of 1%. The following protein inhibitors were also included: 1 μg/ml aprotinin, 10 μg/ml leupeptin, 1 μg/ml pepstatin, and 2 mM PMSF. Lysates were frozen at −80°C. Ten microliters of the protein lysate was analyzed on a 10% SDS-PAGE gel.

ODF1-OIP1 Association Assays

Glutathione beads (Sigma, St. Louis, MO) to which one of the GST-ODF1 fusion proteins was bound were prepared by incubating 300 μl of a bacterial lysate containing the desired GST-ODF1 protein with 100 μl beads (50% v/v in binding buffer) and 10 μM L-methionine for 30 min at 4°C. After incubation, beads were pelleted at 3000 rpm for 5 min, the supernatant was removed, and beads were washed three times with 1 ml of cold PBS. After the final wash, beads were resuspended in a volume of binding buffer equal to that of the pelleted beads and 20 μl was added to the binding reaction. Protein interaction assays were next carried out as follows: 12.5 μl of *Oip1* in vitro translation reaction were added to 20 μl of loaded glutathione beads together with 15 μl of 0.1 M L-methionine and 57.5 μl of binding buffer (20 mM Tris-HCl pH 7.5, 150 mM NaCl, 0.5% NP-40, and 20 mg/ml BSA). The mixture was incubated overnight at 4°C. Reactions were pelleted at 3000 rpm for 5 min and washed three times with 500 μl of wash buffer (20 mM Tris-HCl pH 7.5, 150 mM NaCl, 0.5% NP-40, and 0.05% sarkosyl). All traces of supernatant were removed and 20 μl of sample buffer was added to the beads. Proteins were denatured by heating to 95°C for 5 min

and analyzed on a 15% SDS-PAGE gel. Gel-separated GST-ODF1 fusion proteins were visualized by staining with Coomassie brilliant blue, photographed, and gels were next exposed to x-ray film for 72 h to detect radiolabeled OIP1 protein.

Nucleotide Sequence and Protein Structure Analysis Software

The OIP1 protein sequence was submitted to the Swiss-Model protein modeling site (http://www.expasy.ch/swissmod/) to generate a putative three-dimensional (3-D) OIP1 structure. For protein threading, two templates, equine herpes virus CHC (IEEHV) [21] and human TFIIH Mat1 [22] were submitted along with the OIP1 protein sequence. Omiga 2 software (Accelrys, Burlington, MA) was used to predict protein motifs, perform ClustalW alignments, and analyze the amino acid composition of rat testis OIP1.

OIP1 Gene Expression Analysis by RT-PCR

RNA was isolated from various rat organs and rat testes at different stages of development and used to synthesize cDNA as described above. RT-PCR was carried out using primer pair RatSpR-ContPr (5′-CATGA-ATTCGATAGTCCAAGTCCTAAGAGACAGCG-3′) and R-480SeqPr 1 (5′-GTCGAGACAGACGTTCCCTTC-3′). In indicated instances, a second round of PCR was performed using 1 μl of the initial product as the template for a second set of 30 cycles. The reaction products were analyzed on 1.0% agarose gels.

OIP1 Protein Analysis

Polyclonal rabbit antibodies were raised against a bacterially produced maltose binding protein (MBP)-18-8-1 fusion protein as described previously [11]. The antibodies were affinity-purified by binding them to filter-immobilized MBP-18-8-1 fusion protein as described [14]. Affinity-purified anti-OIP1 antibodies were used 1) in Western blotting experiments to detect testicular OIP1 protein as described [12] using protein extracts isolated from testis, spermatozoa, heart, and smooth muscle; and 2) in indirect immunofluorescence analysis of formaldehyde-fixed, Triton-permeabilized rat epididymal spermatozoa using Cy-3 conjugated goat anti-rabbit sera as described [11, 16].

RESULTS

Isolation of an ODF1-Interacting Protein OIP1

The ODF1 C-terminal contains an evolutionary conserved CGP repeat, which was used in a yeast two-hybrid screen to identify proteins capable of interacting with ODF1. The C-terminal portion of ODF1 was fused to the GAL4 DNA-binding domain (pGBT/CT) and used as bait to screen a rat testis yeast cDNA expression library containing cDNAs fused to the GAL4 transactivation domain [11]. Clone pGAD18-8-1 with an insert of 819 bp was identified and used for further analyses. The plasmid was tested by itself or in combination with ODF1 NT (residues 1–147) and ODF1 CT (residues 147–245). The results shown in Table 1 demonstrate that 18-8-1 does not bind to the GAL4 DNA binding domain (pGBT9) nor does it activate HF7c by itself. pGAD18-8-1 was capable of interacting with the ODF1 CT, albeit weakly, and surprisingly, it also showed binding with the ODF1 NT. The observations in yeast were confirmed in the following in vitro binding experiments. A protein-protein association assay using GST-ODF1 fusion proteins and in vitro-translated

18-8-1 was employed. The 18-8-1 fragment was first subcloned into a pBluescript vector, pKS-ATG [9], engineered to have an in-frame translational start site and next translated in vitro in the presence of [^{35}S]Met. Glutathione agarose beads were loaded with GST or GST/NT and GST/CT fusion proteins and incubated with the 18-8-1 translation product. Protein complex formation was analyzed by SDS-PAGE and autoradiography. Coomassie staining of such gels shows the presence of equal amounts of the GST (27 kDa), GST/NT (42 kDa), or GST/CT (37 kDa) fusion proteins bound to the beads (Fig. 1, top panel). Autoradiography of these gels revealed that 18-8-1 is capable of binding to the CT (Fig. 1, bottom panel, lane 3) as well as to the ODF1 NT (Fig. 1, bottom panel, lane 4), confirming the yeast results. The 18-8-1 protein does not bind to beads (lane 1). Binding of 18-8-1 protein was always higher to the ODF1 NT than to CT. We observed a low level of nonspecific signal comigrating with GST. We determined that this was due to the binding of [^{35}S]Met to GST because the signal (lane 2) could be removed by the addition of L-methionine to the binding reactions (see Fig. 7). We named this novel protein (represented by 18-8-1) OIP1, for ODF1 interacting protein.

Cloning Oip1 cDNAs

The nucleotide sequence of the 18-8-1 insert was determined and indicated the presence of a polyadenylation signal, but the absence of an ATG translational start codon, suggesting that 18-8-1 likely does not represent a full-length *Oip1* cDNA clone. To address this possibility, the 819 bp partial sequence was used as a probe in a Northern analysis of RNA isolated from rat testis. The estimated size of the RNA transcript was approximately 2 kilobases (kb) in size (not shown): thus, approximately 1.2 kb of 5′ sequence remained to be cloned. Primers specific for 18-8-1 were designed and long *Oip1* cDNAs were obtained as follows. First, a λgtll cDNA expression library was screened for *Oip1*-specific clones using PCR as described in *Materials and Methods* resulting in isolation of clone RING600(A), which contained 285 bp of additional 5′ sequence. The 1104-bp *Oip1* sequence was next compared with GenBank database entries. The *Oip1* sequence was homologous to several database entries, including mouse AK006888 (adult male testis cDNA from the RIKEN full-length enriched library [23]), human AK024996 (cDNA from colon), and human 14740319 (cDNA isolated from hypothetical protein FLJ21343, accession XM 017882). After unsuccessful attempts at isolating larger clones for *Oip1* employing rapid amplification of cDNA ends (RACE) and RT-PCR strategies, we used a genomics approach to obtain additional rat testis *Oip1* cDNA sequences. Mouse clone AK006888 sequence information was used to design 5′ primers and RT-PCR was carried out using rat round spermatid cDNA, which resulted in clone R-480. Sequence data from R-480 and other clones were compiled and the available rat testicular *Oip1* cDNA sequence was submitted to GenBank (accession number AF480444). This nucleotide sequence was used to predict the OIP1 protein sequence shown in Figure 2 in a comparison with proteins predicted from human (AK024996 and 14740319) and mouse (AK006888) homologs. The rat OIP1 protein has 432 residues and a predicted molecular weight of 48 700 daltons. The comparison shows that these four proteins are highly similar (>96% identical). The mouse homolog lacks the 90 C-terminal residues shared by the rat and human homologs. The human colon cDNA (AK024996) lacks the indicated Met codon. In several human and mouse cDNA homologs upstream, amino acid residues are present in frame with this Met codon: it is thus likely that the known OIP1-

related sequences are partial. Indeed, Western blot analysis of rat OIP1 suggests that this is the case (see below).

Protein sequence analysis indicated a region with high similarity to the RING finger domain of the H2-subclass C3H2C3 at the OIP1 C-terminus: Figure 3A shows a comparison of the putative OIP1 RING finger motif with the RING finger motifs present in human Ring Finger Protein 6 (RNF6 human; accession number Q9Y252 [24]) and mouse Ring Finger LIM Domain Binding Protein RNFB mouse (accession number Q9WTV7 [25]). The essential cysteine and histidine residues forming the C3H2C3 RING finger are present in OIP1 as indicated (Fig. 3A, underlined). In addition, there is significant conservation of many flanking residues in this region of the proteins (53.6% identity). To obtain further evidence to support the possibility that rat testicular OIP1 contains a RING finger, the OIP1 protein sequence was submitted to the Swiss-Model 3-D modeling site together with the resolved 3-D structures of 1G25 (human TFIIH Mat1 [22] and CHC (equine herpes virus, IEEHV [21]), both confirmed RING finger proteins as folding templates. The result of the protein threading analysis was produced in the format of a Brookhaven structure PDB file, which was analyzed in the RasMol program. The result is shown in Figure 3B in a comparison with the CHC RING motif. It can be seen that the predicted OIP1 RING motif structure is remarkably similar to the CHC RING motif, even though the amino acid identity in the OIP1 and CHC RING regions is only 39%. The C-terminus of the rat testicular OIP1 protein is thus predicted to have the capability to fold as a RING finger motif. The 3-D structure shows three typical β strands forming an antiparallel β sheet and the α helix, all connected by a number of loops. No significant 3-D structure was predicted by the Swiss-Model analysis for the remainder of the OIP1 protein sequence. In addition, no other putative motifs were found using the NCBI domain architecture retrieval tool (DART). We found it interesting that the rat OIP1 protein is very rich in proline residues (15.28% Pro residues; see *Discussion*).

Chromosomal Location and Oip1 Gene Structure Analysis

The rat testis *Oip1* cDNA sequence was analyzed using the NCBI human genome map BLAST algorithm: human *Oip1* is located on chromosome 9, locus p11.2. We next compared the exon-intron structure for the human clones 14740319 and AK024996, mouse clone AK006888, and rat clone *Oip1.* The result is shown in Figure 4. *Oip1* is predicted to have 12 exons and 11 introns spread out over more than 60 kb. Exon 10, which contains the RING finger motif, is, interestingly, absent from mouse clone AK006888, as is exon 2, suggesting that the *Oip1* gene may be subject to differential splicing. The rat *Oip1* sequence contains a putative exon (Fig. 4, indicated by 2*) and is not present in any of the other clones. Furthermore, the 3.66-kb 3′ extension in clone AK024996 is completely co-linear with genomic sequences and ends at an alternative downstream polyadenylation site. It is interesting that the polyadenylation signal used by three of the four mRNAs (TATAAA) differs from the canonical polyadenylation signal sequence AATAAA, whereas the alternative downstream polyadenylation signal used in clone AK024996 is identical to the canonical signal.

Oip1 mRNA Expression Pattern

Preliminary Northern blot analysis of various tissues suggested that *Oip1* is predominantly expressed in testis with most abundant expression in round spermatids (not shown). To analyze whether *Oip1* expression is truly testis-specific, we analyzed *Oip1* mRNA expression patterns by RT-PCR in total RNA isolated from various rat tissues and elutriated pachytene spermatocytes and round spermatids.

The integrity of RNA and cDNA synthesis efficiency were analyzed using β-actin control primers. Figure 5 shows that amplified β-actin fragments are similar for all RNA preparations. The *Oip1* PCR experiment shows that round spermatids and pachytene spermatocytes both express *Oip1* mRNA. *Oip1* mRNA is not present in epididymis. *Oip1* mRNA is also detectable in brain, colon, and lung, with lower levels in kidney, liver, and intestine. No expression was detectable in heart and smooth muscle. When PCR was carried out for an additional 30 cycles, minimal expression was also detected in smooth muscle (not shown). We conclude that *Oip1* exhibits high expression in round spermatids, the major site of ODF1 production, and a lower level of expression in various other tissues.

Expression of Oip1 Begins Early During Spermatogenesis

RT-PCR was employed to assay *Oip1* gene expression during rat testis development. RNA was isolated from the testes of rats at 5, 10, 15, 21, 25, and 31 days of age and was used in RT-PCR assays. Because the first wave of spermatogenesis in the newborn rat is synchronous, this experiment allows identification of germ cells that express *Oip1.* Complementary DNA amount and quality were analyzed using β-actin control primers as described above. Figure 6 shows the results of these assays. It should be noted that RT-PCR experiments as carried out here are not quantitative, and apparent increases or decreases in amplified *Oip1* fragments are only relative to the observed stable level of actin expression. *Oip1* expression begins early during rat spermatogenesis, between Day 5 and Day 10. At this time the germ cell complement of rat testes consists only of dividing spermatogonia. During the first wave of spermatogenesis after birth *Oip1* mRNA levels appear to decrease from Day 10 onward until Day 21, when late pachytene spermatocytes appear. Higher *Oip1* mRNA expression was observed around Day 25 when round spermatids first appear, followed by a decrease in expression (Day 31) when elongating spermatids differentiate. Higher expression levels of *Oip1* are observed in adult rat testis, which contains all germ cells at all stages of differentiation and development. The observed pattern indicates differential *Oip1* expression during spermatogenesis.

OIP1 Localizes to the Sperm Tail

We determined that *Oip1* mRNA is expressed in spermatids, the major site of ODF1 synthesis. To analyze OIP1 protein expression we generated anti-OIP1 antibodies. Affinity-purified polyclonal anti-OIP1 antisera were first used to analyze OIP1 protein in Western blot assays. Figure 7 shows that in testis a peptide of approximately 70 kDa is detected (lane 1), which is not expressed in smooth muscle or heart (lanes 2 and 3), tissues that are also negative for *Oip1* mRNA (see Fig. 5). We also observed a similar pattern using protein extracted from rat spermatozoa (lane 4), but not using preimmune antisera (lane 5). Other, smaller peptides can also be observed, which may result from alternative splicing events.

The Western blot result confirmed our expectation that the likely *Oip1* nucleotide sequence known to date is partial because it predicts a 49-kDa peptide.

We next used the affinity-purified antiserum in immunofluorescence assays of rat epididymal spermatozoa to localize OIP1 protein. The result is shown in Figure 8. Panels a and c show 4′-6′-diamidino-2-phenylindole (DAPI)-stained samples of sperm and panels b and d show the corresponding OIP1-staining patterns. The results show that OIP1 protein is expressed in sperm tails, but not in sperm heads (arrows, panels c and d), with a distribution remarkably similar to those observed for ODF1 [16], and Odf2 [11]: staining is predominant in the sperm midpiece (arrowheads, panels c and d). In control experiments we showed that blocking of the affinity-purified antibodies by preincubation with MBP-18-8-1 fusion protein completely prevented OIP1 staining (panels e and f). This antiserum has not been useful in immunoelectron microscopy, and we do not know at present whether OIP1 is an integral ODF protein, such as ODF1 and Odf2, or whether it is an ODF-associated protein such as Spag4 [14].

OIP1 RING Finger Plays a Role in Interactions with Odf1

To investigate the involvement of the putative RING finger motif in the interaction of OIP1 with ODF1, protein association assays were carried out in vitro and in yeast with an OIP1 construct lacking the RING finger motif. The binding of in vitro translated 18-8-1 OIP1 protein and OIP1 RING deletion mutant to ODF1 NT and CT and to additional ODF1 fragments (ΔNT; residues 1–100), NTΔzip (residues 25–147), and ΔCT (residues 147–201) was tested as described above. Glutathione beads were loaded with the desired GST-ODF1 fusion protein and incubated with in vitro-translated OIP1 proteins. Protein complexes were analyzed by SDS-PAGE. The results of the binding assays are shown in Figure 9. Coomassie staining of gels confirmed the presence of equal amounts of GST-ODF1 fusion proteins (not shown). Control lanes containing only GST show that OIP1 and the OIP1 RING deletion proteins fail to bind to the GST moiety (lanes 1 and 7). OIP1 binds strongly to ODF1 NT (which contains the 145 residue N-terminal half of ODF1) and weakly to ODF1 CT (lanes 2 and 5, respectively), as described above. Strong association was also observed between OIP1 and ODF1 N-terminal fragments containing only the first 100 residues (lane 3) or lacking the ODF1 leucine zipper (lane 4). From this result we conclude that the ODF1 leucine zipper is not involved in binding to OIP1, a result that agrees with the failure to pick up OIP1 in our previous yeast two-hybrid screening assays using the ODF1 leucine zipper as bait. The ODF1 ΔCT fragment, retaining half the CGP repeats, exhibits binding to OIP1 comparable to that of the CT fragment (lane 6 and 5, respectively). Using the OIP1 RING finger deletion mutant in these binding experiments, we observed a drastic reduction in binding between OIP1 and all the ODF1 fusion proteins (Fig. 9, lanes 8–12). Quantitation of the binding interactions is indicated below the autoradiography data in Figure 9. The band intensities were normalized against the GST control lanes. These results clearly indicate that deletion of the OIP1 RING finger reduces the binding of OIP1 to ODF1 NT and CT fragments by a factor of 4-fold to 19-fold.

The ability of the OIP1 RING finger deletion mutant to bind ODF1 NT and CT was also analyzed in yeast (see Table 1). The results in yeast reflect the in vitro binding data, with

decreased or absent binding to CT and reduced binding to NT. The yeast system did not show the stronger in vitro binding of OIP1 to NT compared to CT, but it should be noted that it is not a quantitative system.

DISCUSSION

The morphogenesis and protein composition of sperm tail ODFs have been well characterized, but we are only beginning to characterize the individual components underlying this sperm structure and their interactions. ODF1 and Odf2 have been independently isolated and characterized by several laboratories [7, 8, 10, 11, 26]. To approach the possible protein interactions that play a role in sperm tail development we had previously used a screen of a rat testis yeast two-hybrid libraries using the N-terminal leucine zipper of ODF1, which resulted in the isolation of Odf2 [11], Spag4 [14], and more recently, Spag5 [15]. Their characterization demonstrates a temporal order of synthesis, specific protein interaction patterns mediated by leucine zippers, and specific localization to different sperm tail structures. Spag4 localizes to the axoneme and manchette, both microtubule-containing structures, and we proposed that in association with ODF1 it serves as a link between the developing ODF and axoneme [14, 27]. Recently, a third ODF protein, Odf3, has been reported [28, 29]. Interactions between ODF proteins and ODF-associated proteins suggest that a highly intricate network of protein interactions exists that are required for development of a functional sperm.

Our previous characterization of ODF1 suggested that it is able to mediate self-interaction via the N-terminal leucine zipper as well as via its C-terminal portion [11]. It is interesting that the ODF1 CT harbors CGP repeats that are found conserved in *Drosophila Mst(3)* proteins, which localize to *Drosophila* sperm tail fibers. Indeed, this evolutionary conserved sequence has been exploited to isolate mammalian ODF1 [26]. Based on these data we used the ODF1 C-terminus in a yeast two-hybrid library screen to isolate interacting proteins, which resulted in the isolation of a novel ODF1 interacting protein, OIP1. When the isolated *Oip1* clone (pGAD18-8-1) was tested in yeast, we verified that OIP1 interacts with the ODF1 CT. Unexpectedly it also showed binding to ODF1 NT. Although the yeast system is not quantitative, we estimated, based on the number and size of growing yeast colonies, that both interactions are weak in comparison to strong interactions such as the one between ODF1 and Odf2. OIP1 had not been isolated before using the N-terminal leucine zipper as bait, suggesting that the ODF1 leucine zipper does not play a role in the interaction between OIP1 and ODF1 NT. This was confirmed in in vitro binding experiments between various GST-ODF1 fusion proteins and in vitro translated OIP1. OIP1 can associate with both ODF1 NT and CT, and with a leucine zipper deletion mutant of the ODF1 NT (NTΔzip). The use of various deletion mutants indicates that OIP1 probably binds to the ODF1 N-terminus between residues 25 and 100. The binding between OIP1 and NT is stronger than with CT. One possible explanation for the differential binding strength may be that ODF1 NT dimers (leucine zipper mediated) can still efficiently bind OIP1, whereas ODF1 CT dimers (employing the same CGP repeats that associate with OIP1) cannot. Be it as it may, our results clearly show that OIP1 can bind to two different regions in ODF1.

Sequence analysis of the original *Oip1* clone together with Northern blot analyses revealed that 5′ sequences were missing from the clone. Several approaches were pursued to obtain additional 5′ *Oip1* sequence information, including specific RT-PCR assays based on database searches. Several cDNAs with significant similarity to rat *Oip1* were identified in the databases, some of which contained extended 5′ regions, implying there might be additional 5′ sequences. Comparison of the predicted protein sequences (Fig. 2) indicates a very high degree of identity (>96%) between several human, mouse, and rat OIP1 proteins. At this point we believe it likely that a start codon exists in *Oip1* mRNA upstream of the indicated Met codon of rat OIP1, because the antibodies raised against OIP1 detected a larger peptide in Western blot assays. The anti-OIP1 antisera also demonstrated that this protein shows localization in epididymal sperm tails similar to that previously determined for ODF1 and Odf2. Further analyses will establish the subcellular localization of OIP1 with respect to the ODF.

Analysis of OIP1 predicts the presence of a RING finger of the subclass $C_3H_2C_3$ at its very C-terminus. Also, the region upstream of the putative RING finger is very rich in proline residues. A comparison between the RING finger motifs of two RING proteins and rat OIP1 (Fig. 2B) shows that the spacing of essential cysteine and histidine residues that make up the motif, as well as many flanking residues, are highly conserved. RING fingers are part of a zinc binding family of proteins including TRIADs [30], LIMs, and LAP fingers [31]. The distinguishing feature of a RING finger is its ability to bind two zinc atoms in a unique cross-braced structure [31]. Based on coordination the 80 members of the RING finger protein family are classified as C_3HC_4 fingers, C_4C_4, and $C_2H_2C_4$ [31, 32]. The structure of two RING fingers, PML [33] and IEEHV CHC [21], has been resolved using nuclear magnetic resonance. Outside the conserved amino acids in the RING finger, these two proteins share only 15% homology [34]. Submission of OIP1 to the Swiss modeling protein database together with possible templates (IEEHV CHC and TFIIH Mat 1) resulted in the prediction of an OIP1 3-D structure strongly resembling the RING finger structure containing three β sheets and one α helix. Outside of the putative RING finger, no significant structural homology was found.

The RING domain is present in proteins with very diverse functions such as oncogenesis, viral pathogenicity, and signal transduction that are commonly found in multiprotein complexes [34, 35]. RING fingers are candidates for E3 ubiquitin-protein ligases: they mediate binding activity toward E2 ubiquitin-conjugating enzymes [36]. Several RING fingers (Praja 1, NF-X1, TRC8, and kf-1) indeed displayed E2-dependent ubiquitination activity in vitro, which was lost upon mutation of RING cysteines [36]. It is not known whether the OIP1 RING finger confers the ability to mediate ubiquitination in addition to having other cellular roles.

Further analysis of the *Oip1* sequence shows that it maps to human chromosome 9 at position 9p11.2. The genomic organization predicted for human *Oip1* suggests that *Oip1* has at least 12 exons and 11 introns. Comparison of exon-intron structures suggested that differential splicing as well as alternative use of polyadenylation sites regulates *Oip1* gene expression. For example, the mouse homolog lacks exons 2 and 10 (Fig. 4) and the human clone AK024996 uses a downstream polyadenylation site adding approximately 3.66 kb of

3′ untranslated region to the mRNA. All cDNA clones contain exons 3–9, and 11. In the mouse, cDNAs have been reported that do not contain exon 10. This may be important because this exon contains the coding information for the RING finger motif. Removal of exon 10 by differential splicing results in the absence of the RING finger (see Fig. 2, AK006888), which we demonstrate here has repercussions for the interaction of the variant OIP1 protein; an OIP1 RING deletion dramatically reduced its ability to bind ODF1. Residual binding to ODF1 NT and CT was observed that may occur through other OIP1 sequences. During the course of our efforts to clone longer rat *Oip1* cDNAs by RT-PCR we identified an additional natural variant that lacks the proline rich region (not shown), suggesting that this region may play a functional role.

Analysis of the *Oip1* expression pattern by RT-PCR demonstrated *Oip1* mRNA in male germ cells, with highest testicular expression in round spermatids. No *Oip1* mRNA was detectable by RT-PCR in epididymis. *Oip1* is not a testis-specific gene because its expression could be detected in several somatic tissues, albeit at a lower level. The expression of *Oip1* was also analyzed in developing testes. An unusual pattern was consistently observed that might reflect that certain male germ cells at certain stages of development express high levels of *Oip1* (such as round spermatids), whereas other germ cells (e.g., elongating spermatids) produce much lower levels of *Oip1* mRNA. Onset of testicular *Oip1* transcription is between 6 and 10 days after birth, well before the presence of early pachytene spermatocytes, strongly suggesting that *Oip1* is active in mitotically dividing spermatogonia. The function of *Oip1* in spermatogenesis remains to be determined, but the high expression levels of both OIP1 and ODF1 during spermio-genesis suggest that their association—possibly in part mediated by the RING finger sequence—may have functional significance. The precise role of OIP1 remains to be elucidated.

In concert with our previous ODF1 interaction, results of our current data suggest a molecular networking model in which ODF1 may act as a central linking peptide in ODFs. ODF1 has two distinct protein interaction domains that mediate highly specific protein-protein interactions. As well, ODF1 can self-interact. Thus, we propose that ODF1 plays a role in sperm tail morphogenesis by providing the basis of a complex protein network.

Acknowledgments

We thank Dr. X. Shao and H. Tarnasky for help with the initial yeast two-hybrid screening assays and Dr. B. Bhullar for comments and suggestions. We thank Dr. M.H. Modarressi for a gift of rat testis RNAs.

References

1. Fawcett DW. The mammalian spermatozoon. Dev Biol. 1975; 44:394–436. [PubMed: 805734]
2. Olson GE, Sammons DW. Structural chemistry of outer dense fibers of rat sperm. Biol Reprod. 1980; 22:319–332. [PubMed: 7378538]
3. Calvin HI. Isolation of subfractionation of mammalian sperm heads and tails. Methods Cell Biol. 1976; 13:85–104. [PubMed: 772365]
4. Vera JC, Brito M, Zuvic T, Burzio LO. Polypeptide composition of rat sperm outer dense fibers. A simple procedure to isolate the fibrillar complex. J Biol Chem. 1984; 259:5970–5977. [PubMed: 6715381]

5. Oko R. Comparative analysis of proteins from the fibrous sheath and outer dense fibers of rat spermatozoa. Biol Reprod. 1988; 39:169–182. [PubMed: 3207795]
6. Baltz JM, Williams PO, Cone RA. Dense fibers protect mammalian sperm against damage. Biol Reprod. 1990; 43:485–491. [PubMed: 2271730]
7. van der Hoorn FA, Tarnasky HA, Nordeen SK. A new rat gene RT7 is specifically expressed during spermatogenesis. Dev Biol. 1990; 142:147–154. [PubMed: 1699827]
8. Morales CR, Oko R, Clermont Y. Molecular cloning and developmental expression of an mRNA encoding the 27 kDa outer dense fiber protein of rat spermatozoa. Mol Reprod Dev. 1994; 37:229–240. [PubMed: 8179907]
9. Shao X, van der Hoorn FA. Self-interaction of the major 27-kilodalton outer dense fiber protein is in part mediated by a leucine zipper domain in the rat. Biol Reprod. 1996; 55:1343–1350. [PubMed: 8949892]
10. Burfeind P, Hoyer-Fender S. Sequence and developmental expression of a mRNA encoding a putative protein of rat sperm outer dense fibers. Dev Biol. 1991; 148:195–204. [PubMed: 1936558]
11. Shao X, Tarnasky HA, Schalles U, Oko R, van der Hoorn FA. Interactional cloning of the 84-kDa major outer dense fiber protein Odf84. Leucine zippers mediate associations of Odf84 and Odf27. J Biol Chem. 1997; 272:6105–6113. [PubMed: 9045620]
12. Schalles U, Shao X, van der Hoorn FA, Oko R. Developmental expression of the 84-kDa ODF sperm protein: localization to both the cortex and medulla of outer dense fibers and to the connecting piece. Dev Biol. 1998; 199:250–260. [PubMed: 9698445]
13. Nakagawa Y, Yamane Y, Okanoue T, Tsukita S, Tsukita S. Outer dense fiber 2 is a widespread centrosome scaffold component preferentially associated with mother centrioles: its identification from isolated centrosomes. Mol Biol Cell. 2001; 12:1687–1697. [PubMed: 11408577]
14. Shao X, Tarnasky HA, Lee JP, Oko R, van der Hoorn FA. Spag4, a novel sperm protein, binds outer dense-fiber protein ODF1 and localizes to microtubules of manchette and axoneme. Dev Biol. 1999; 211:109–123. [PubMed: 10373309]
15. Shao X, Xue J, van der Hoorn FA. Testicular protein Spag5 has similarity to mitotic spindle protein Deepest and binds outer dense fiber protein ODF1. Mol Reprod Dev. 2001; 59:410–416. [PubMed: 11468777]
16. Higgy NA, Pastoor T, Renz C, Tarnasky HA, van der Hoorn FA. Testis-specific RT7 protein localizes to the sperm tail and associates with itself. Biol Reprod. 1994; 50:1357–1366. [PubMed: 7521678]
17. Kuhn R, Kuhn C, Borsch D, Glatzer KH, Schafer U, Schafer M. A cluster of four genes selectively expressed in the male germ line of *Drosophila melanogaster*. Mech Dev. 1991; 35:143–151. [PubMed: 1684716]
18. Kuhn R, Schafer U, Schafer M. Cis-acting regions sufficient for spermatocyte-specific transcriptional and spermatid-specific translational control of the *Drosophila melanogaster* gene mst(3)gl-9. EMBO J. 1988; 7:447–454. [PubMed: 2835228]
19. Schafer M, Borsch D, Hulster A, Schafer U. Expression of a gene duplication encoding conserved sperm tail proteins is translationally regulated in *Drosophila melanogaster*. Mol Cell Biol. 1993; 13:1708–1718. [PubMed: 8441407]
20. Frangioni JV, Neel BG. Solubilization and purification of enzymatically active glutathione S-transferase (pGEX) fusion proteins. Anal Biochem. 1993; 210:179–187. [PubMed: 8489015]
21. Barlow PN, Luisi B, Milner A, Elliott M, Everett R. Structure of the C3HC4 domain by 1H-nuclear magnetic resonance spectroscopy. A new structural class of zinc-finger. J Mol Biol. 1994; 237:201–211. [PubMed: 8126734]
22. Gervais V, Busso D, Wasielewski E, Poterszman A, Egly JM, Thierry JC, Kieffer B. Solution structure of the N-terminal domain of the human TFIIH MAT1 subunit: new insights into the RING finger family. J Biol Chem. 2001; 276:7457–7464. [PubMed: 11056162]
23. Carninci P, Hayashizaki Y. High-efficiency full-length cDNA cloning. Methods Enzymol. 1999; 303:19–44. [PubMed: 10349636]

24. Macdonald DH, Lahiri D, Sampath A, Chase A, Sohal J, Cross NC. Cloning and characterization of RNF6, a novel RING finger gene mapping to 13q12. Genomics. 1999; 58:94–97. [PubMed: 10331950]
25. Bach I, Rodriguez-Esteban C, Carriere C, Bhushan A, Krones A, Rose DW, Glass CK, Andersen B, Izpisua Belmonte JC, Rosenfeld MG. RLIM inhibits functional activity of LIM homeodomain transcription factors via recruitment of the histone deacetylase complex. Nat Genet. 1999; 22:394–399. [PubMed: 10431247]
26. Brohmann H, Pinnecke S, Hoyer-Fender S. Identification and characterization of new cDNAs encoding outer dense fiber proteins of rat sperm. J Biol Chem. 1997; 272:10327–10332. [PubMed: 9092585]
27. Kierszenbaum AL. Spermatid manchette: plugging proteins to zero into the sperm tail. Mol Reprod Dev. 2001; 59:347–349. [PubMed: 11468770]
28. Petersen C, Aumuller G, Bahrami M, Hoyer-Fender S. Molecular cloning of Odf3 encoding a novel coiled-coil protein of sperm tail outer dense fibers. Mol Reprod Dev. 2002; 61:102–112. [PubMed: 11774381]
29. Kierszenbaum AL. Keratins: unraveling the coordinated construction of scaffolds in spermatogenic cells. Mol Reprod Dev. 2002; 61:1–2. [PubMed: 11774369]
30. van der Reijden BA, Erpelinck-Verschueren CA, Lowenberg B, Jansen JH. TRIADs: a new class of proteins with a novel cysteine-rich signature. Protein Sci. 1999; 8:1557–1561. [PubMed: 10422847]
31. Borden KL, Freemont PS. The RING finger domain: a recent example of a sequence-structure family. Curr Opin Struct Biol. 1996; 6:395–401. [PubMed: 8804826]
32. Hanzawa H, de Ruwe MJ, Albert TK, Der Vliet PC, Timmers HT, Boelens R. The structure of the C4C4 ring finger of human NOT4 reveals features distinct from those of C3HC4 RING fingers. J Biol Chem. 2001; 276:10185–10190. [PubMed: 11087754]
33. Borden KL, Boddy MN, Lally J, O'Reilly NJ, Martin S, Howe K, Solomon E, Freemont PS. The solution structure of the RING finger domain from the acute promyelocytic leukaemia proto-oncoprotein PML. EMBO J. 1995; 14:1532–1541. [PubMed: 7729428]
34. Saurin AJ, Borden KL, Boddy MN, Freemont PS. Does this have a familiar RING? Trends Biochem Sci. 1996; 21:208–214. [PubMed: 8744354]
35. Copps K, Richman R, Lyman LM, Chang KA, Rampersad-Ammons J, Kuroda MI. Complex formation by the *Drosophila* MSL proteins: role of the MSL2 RING finger in protein complex assembly. EMBO J. 1998; 17:5409–5417. [PubMed: 9736618]
36. Lorick KL, Jensen JP, Fang S, Ong AM, Hatakeyama S, Weissman AM. RING fingers mediate ubiquitin-conjugating enzyme (E2)-dependent ubiquitination. Proc Natl Acad Sci U S A. 1999; 96:11364–11369. [PubMed: 10500182]

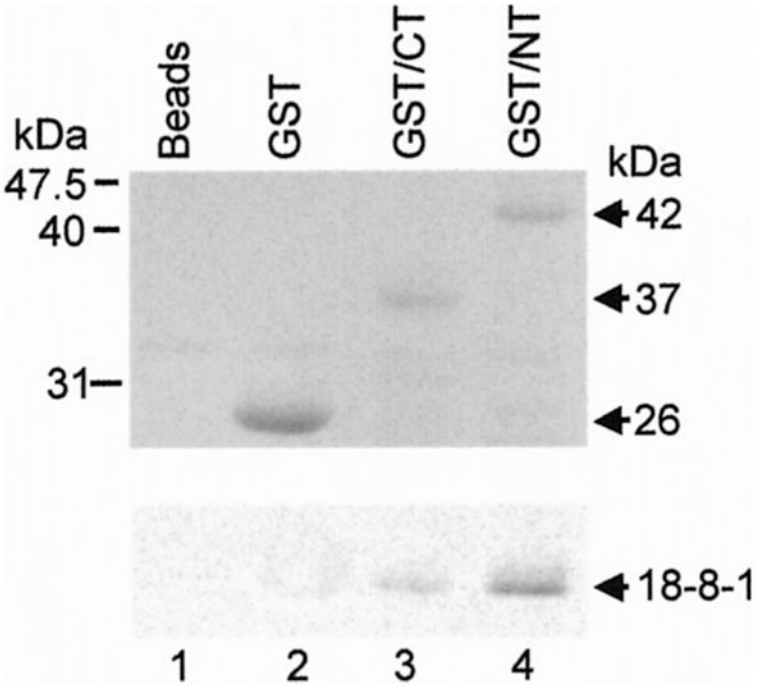

FIG. 1.

In vitro association of OIP1 and ODF1. Glutathione beads were used either direct (lane 1) or after loading with GST, GST/CT, and GST/NT ODF1 fusion proteins (lanes 2–4) in binding assays with in vitro-translated, radiolabeled OIP1 protein. Protein complexes were analyzed by SDS-PAGE. The top panel shows the resulting protein staining pattern of the GST fusion proteins. The bottom panel shows an autoradiograph of the same gel, indicating binding of the OIP1 protein to both the ODF1 N-terminus and C-terminus.

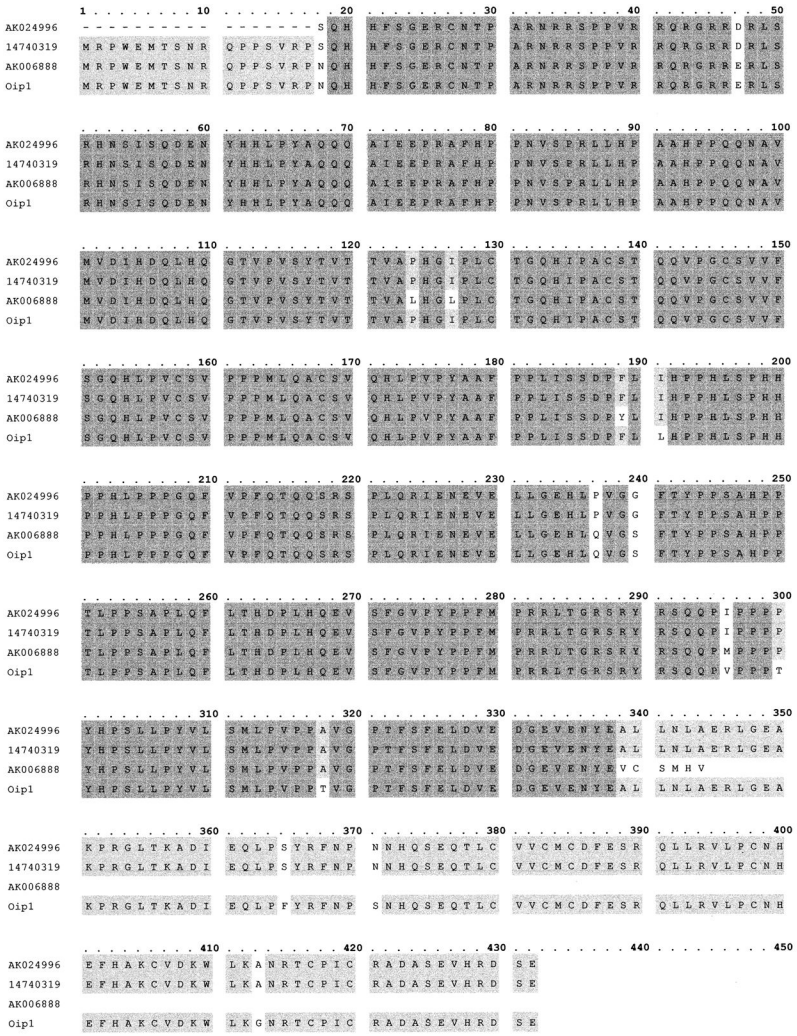

FIG. 2.

Sequence comparison between rat testicular OIP1 and related proteins. The rat OIP1 amino acid sequence was compared to those predicted for the human AK024996 (colon) and 14740319 (hypothetical protein FLJ21343) cDNAs and the mouse AK006888 (adult testis) cDNA. Note the extensive identity. The mouse AK006888 protein lacks the C-terminus present in the rat and human proteins. The human AK024996 protein lacks the indicated Met codon.

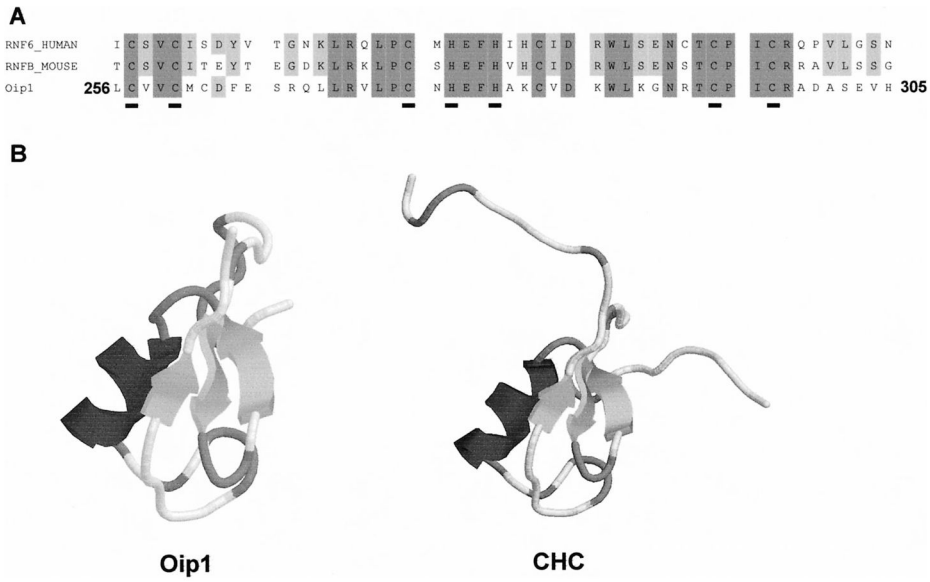

FIG. 3.

Rat OIP1 harbors a RING finger motif. **A**) Sequence analysis of rat OIP1 indicated that its C-terminus harbors the RING finger motif of the H2 subclass. Shown is a comparison between this region of rat OIP1 (amino acids 256–305) and the otherwise completely unrelated RING finger proteins RNF6 human and RNFB mouse. The essential cysteine and histidine residues are underlined. Note that besides these essential residues, several flanking amino acids are also conserved (53.6% identity). **B**) To analyze whether this region of OIP1 can indeed fold as a RING finger, the OIP1 protein sequence was submitted to the Swiss-Model 3-D structure prediction program. The result for rat OIP1 is shown in a comparison with the structure of the equine herpes CHC RING finger protein. Note the high degree of similarity between the relative orientation of the three β sheets and α helix between the OIP1 and CHC 3-D protein structures.

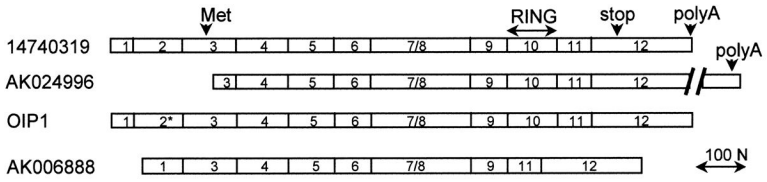

FIG. 4.

Exon structure of rat *Oip1* and related human and mouse cDNAs. The cDNA sequences for rat *Oip1,* human 14740319 and AK024996 genes, and mouse AK006888 gene were mapped to the human 300-kb genomic 16180809 sequence of chromosome 9, region p11.2. Exon-intron structures were determined using Omiga 2 software and shown are the order of exons in the four cDNAs. Indicated are the first identified Met codon (see Fig. 2), the RING finger sequences in exon 10, the location of the translation stop codon in exon 12 and the two polyadenylation sites observed in different cDNAs. Note that the human AK024996 cDNA lacks the Met codon and that mouse AK006888 cDNA lacks exon 2 as well as exon 10. Rat *Oip1* cDNA contains a sequence (indicated as 2*) not found in the other cDNAs.

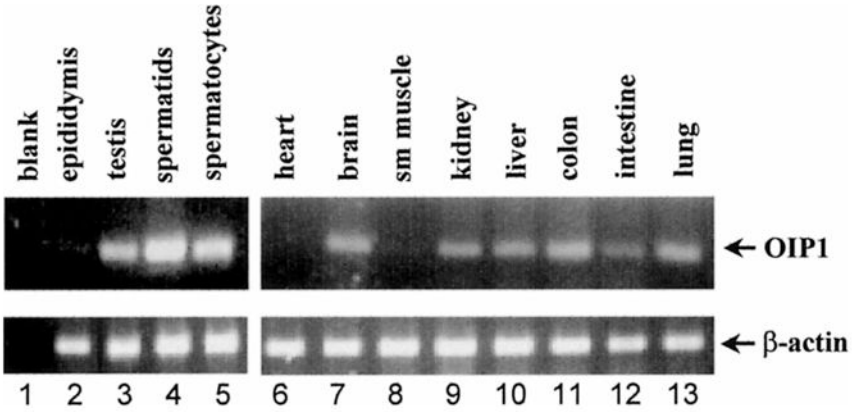

FIG. 5.

Oip1 is expressed in male germ cells as well as somatic tissues. The *Oip1* mRNA expression pattern was analyzed by RT-PCR using *Oip1*-specific primers (top panels). RNA was isolated from the indicated tissues and cells and converted to cDNA. Round spermatids and pachytene spermatocytes were isolated by centrifugal elutriation. Quality and quantity of cDNAs were investigated using β-actin specific primers (bottom panels). Note the absence of *Oip1* mRNA in epididymis, heart, and smooth muscle. Relatively high levels of expression were detected in round spermatids and pachytene spermatocytes. Lane 1 shows a water control (blank).

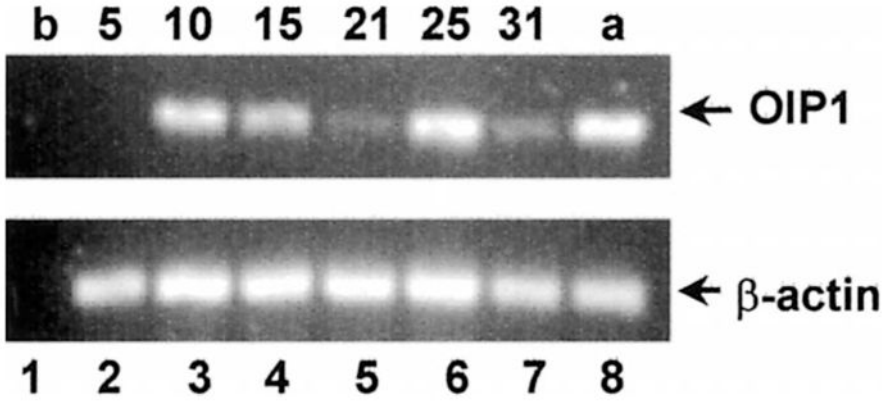

FIG. 6.

Oip1 mRNA levels vary during male germ cell development. *Oip1* mRNA expression was analyzed by RT-PCR using *Oip1*-specific primers (top panel) in rat testes isolated at indicated times after birth (5, 10, 15, 21, 25, and 31 days) and from adult rat testis (**a**). Lane 1 (**b**) shows the result of RT-PCR analysis on negative water sample control. Quality and quantity of cDNAs were investigated using β-actin specific primers (bottom panel). Note that rat testicular *Oip1* mRNA is first detectable in 10-day-old testis (indicating *Oip1* mRNA expression in spermatogonia), and that *Oip1* mRNA levels vary significantly during the first wave of spermatogenesis after birth. Maximal expression at 25 days after birth coincides with the appearance of round spermatids.

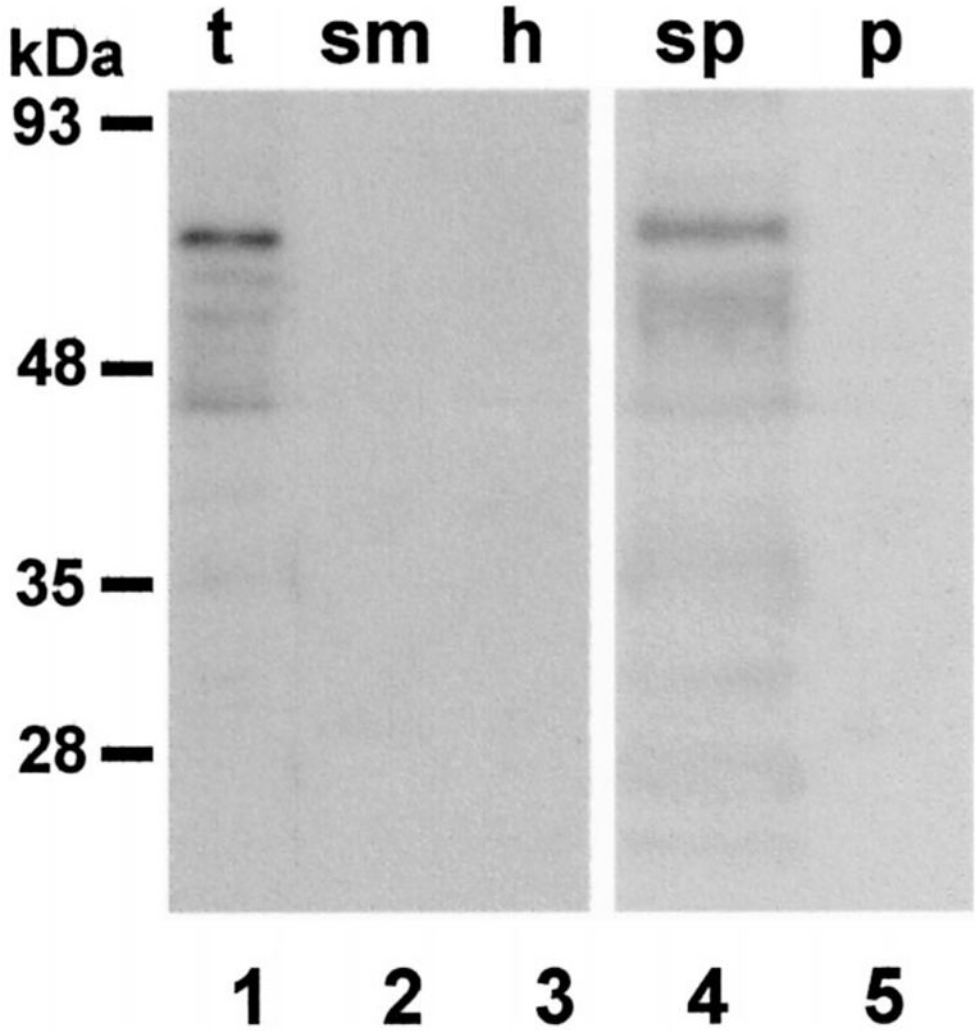

FIG. 7.

OIP1 protein expression. Affinity-purified anti-OIP1 antibodies were prepared and used in Western blot analyses of electrophoretically separated, immobilized proteins isolated from testis (t), smooth muscle (sm), heart (h), and spermatozoa (sp) (lanes 1–4, respectively). Extracts from spermatozoa were also analyzed using preimmune sera (p) (lane 5). Molecular weight markers are indicated. Note that smooth muscle and heart lack *Oip1* mRNA expression, as determined by RT-PCR.

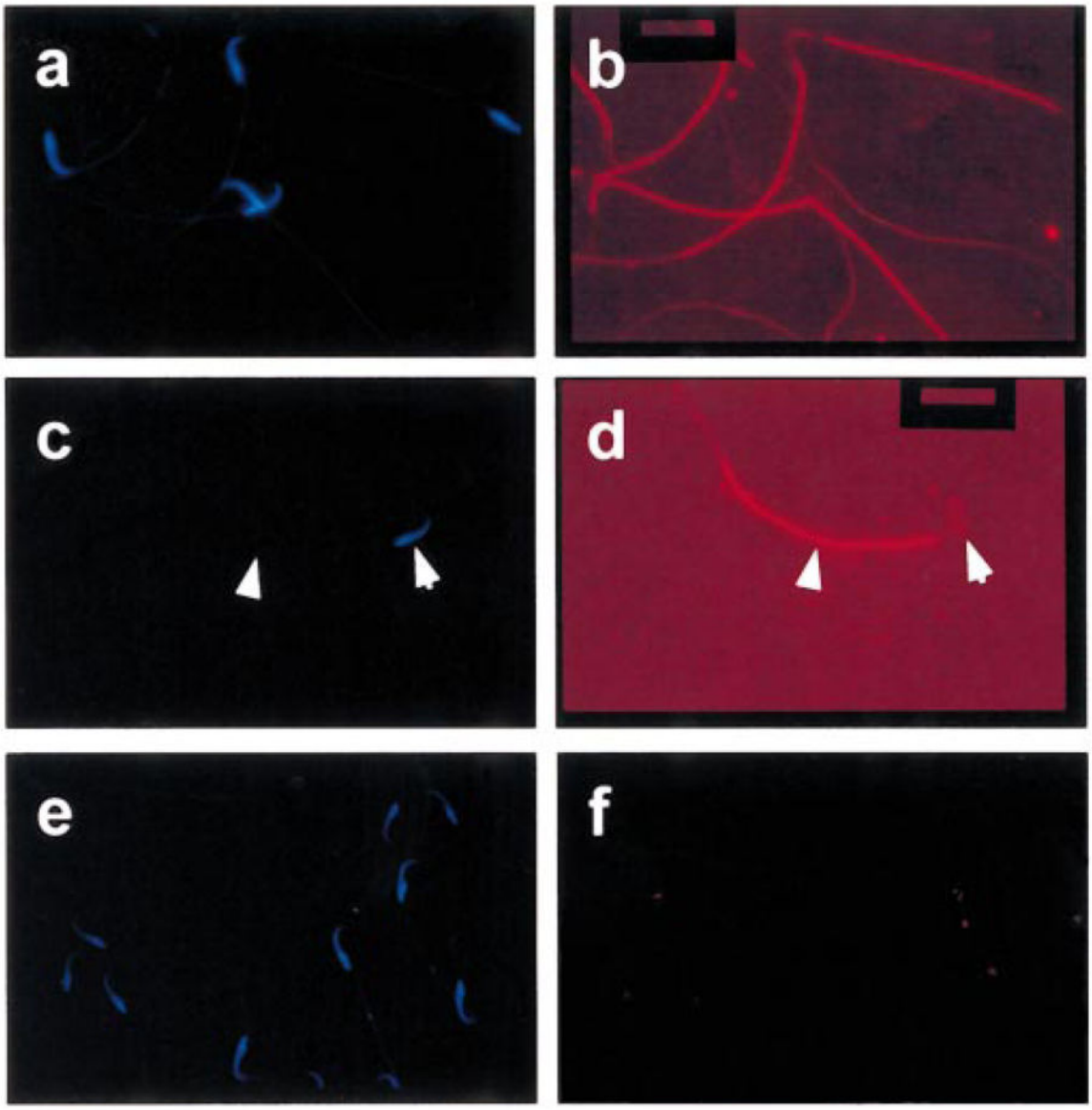

FIG. 8.

OIP1 peptide localizes to sperm tails. To localize OIP1 protein we used fixed rat epididymal spermatozoa in indirect immunofluorescence assays. Sperm were incubated directly with affinity-purified anti-OIP1 antibodies (**a**–**d**) or with affinity-purified anti-OIP1 antibodies that had been preincubated with MBP-18-8-1 in blocking experiments (**e** and **f**). Primary antibodies were visualized by incubation with Cy3-conjugated goat anti-rabbit secondary antibodies, and examined at a magnification of ×100. **a**, **c**, and **e**) DAPI-stained spermatozoa; **b**, **d**, and **f**) OIP1 protein staining pattern. Note that OIP1 specifically localizes to the tail (arrowheads), not head (arrows).

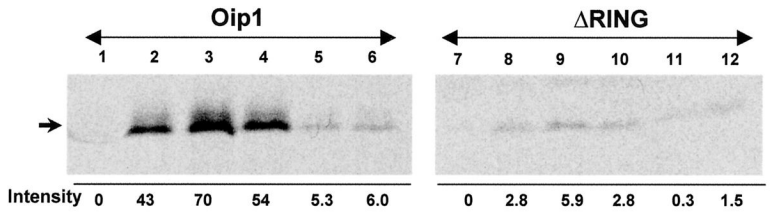

FIG. 9.

OIP1 RING finger sequences are involved in ODF1 binding. A ΔRING finger deletion mutant of OIP1 was constructed and tested together with OIP1 for in vitro binding capability to various GST-ODF1 fusion proteins. Glutathione beads were loaded with GST (lanes 1 and 7), GST/NT (lanes 2 and 8), GST/ΔNT (lanes 3 and 9), GST/NTΔzip (lanes 4 and 10), GST/CT (lanes 5 and 11), and GST/ΔCT (lanes 6 and 12). Next they were incubated with in vitro translated and radiolabeled rat OIP1 (lanes 1–6) or ΔRING (lanes 7–12). Protein complexes were analyzed by SDS-PAGE and autoradiography. Bound OIP1 proteins are indicated (arrow). Band intensities were quantified and normalized to the signal obtained for GST (lanes 1 and 7) to obtain the indicated relative amounts of bound OIP1. Note that deletion of the putative RING finger sequences significantly reduced OIP1 binding to ODF1 proteins.

TABLE 1

Analysis of ODF1 interactions with the novel protein OIP1 encoded by pGAD18-8-1 cDNA in yeast strain HF7c.

	GAL4 DBD hybrid plasmids†			
	none	**pGBT9**	**pGBT/CT‡**	**pGBT/NT‡**
pGAD18-8-1*	−	−	+	+
pGADΔRING	−	−	−	+/−

*OIP1 expression constructs were tested in yeast strain HF7c by themselves or in combination with the indicated GAL4 DBD constructs: growth of yeast colonies on $Leu^{-}His^{-}Trp^{-}$ plates was analyzed. +/− denotes limited growth of yeast colonies in reduced numbers.

†Indicated are the GAL4 DNA binding domain constructs.

‡pGBT/CT and pGBT/NT express GAL4 DBD fusion proteins with ODF1 C-terminus and N-terminus, respectively.